# Structural and Topological Studies of Methionine Radical Cations in Dipeptides: Electron Sharing in Two-Center Three-Electron Bonds

**ARTICLE** *in* THE JOURNAL OF PHYSICAL CHEMISTRY A · JULY 2010

Impact Factor: 2.69 · DOI: 10.1021/jp911983a · Source: PubMed



**3 AUTHORS**, INCLUDING:

Isabelle Fourré
Sorbonne universités, UPMC - Paris 6
**16** PUBLICATIONS **274** CITATIONS
SEE PROFILE

Chantal Houée-Levin
Université Paris-Sud 11
**125** PUBLICATIONS **1,560** CITATIONS
SEE PROFILE

# Structural and Topological Studies of Methionine Radical Cations in Dipeptides: Electron Sharing in Two-Center Three-Electron Bonds

**Isabelle Fourré,*,†,‡ Jacqueline Bergès,†,‡,§ and Chantal Houée-Levin||**

*Université Pierre et Marie Curie, UMR 7616, Laboratoire de Chimie Théorique, F-75005 Paris, France, CNRS, UMR 7616, Laboratoire de Chimie Théorique, F-75005 Paris, France, Université Paris Descartes, F-75006 Paris, France, and Université Paris Sud, UMR 8000, Laboratoire de Chimie Physique, F-91405 Orsay, also at CNRS F-91405 Orsay, France*

*Received: December 18, 2009; Revised Manuscript Received: April 6, 2010*

One electron oxidation of methionine in peptides is highly dependent on the local structure. The sulfur-centered radical cation can complex with oxygen, nitrogen, or other sulfur atoms from a neighboring residue or from the peptidic bond, forming an intramolecular S∴X two-center three-electron bond (X = S, N, O). This stabilization was investigated computationnally in the radical cations of three peptides, methionine glycine (Met Gly) and its reverse sequence Gly Met, and Met Met. Geometry optimizations were done at the BH&HLYP/6-31G(d) level of theory and the effect of solvation was taken into account using a continuum model (CPCM). Up to seven stable conformations were considered for each peptide, with formation of 5−10 member cycles involving nitrogen from the peptidic bond or from the amine, oxygen from the peptidic bond or from the carboxylate group, or sulfur from the other residue for Met Met. The absorption wavelengths corresponding to the $\sigma \rightarrow \sigma^*$ transition calculated for each complex at the TD-BH&HLYP/6-311+G(d,p)//BH&HLYP/6-31G(d) level of theory vary from the near-UV for the S∴O bonds to the green visible for the S∴S bonds. For X = N, they increase with the SN distance as expected for a 2c−3e bond, whereas for X = O they slightly decrease. Characterization of these 2c−3e bonds as a function of the sequence, using the ELF and the AIM topological analyses, shows the different natures of the S∴X bonds, which is purely 2c−3e for X = S, mainly 2c−3e with a part of electrostatic interaction for X = N and mainly electrostatic for X = O.

## I. Introduction

Methionine (Met) is an essential amino acid with a thioether function. In oxidative stress, it is one of the major targets for protein or peptide oxidation by oxygen or nitrogen free radicals owing to the presence of the sulfur.[1] This oxidation leads most frequently to methionine sulfoxide in both enantiomeric forms *R* and *S* (abbreviated MetSO). This process might play a role in redox homeostasis and in prevention of irreversible modifications,[2] since methionine sulfoxide reductase can regenerate Met. Thus this amino acid could act as a molecular switch to detoxify oxidants and protect important regions of the protein.[3] However when it is not repaired, its oxidation is a highly damaging event associated to pathogenesis and to the aging process. For instance it is linked to the neurotoxicity of $\beta$ amyloid peptide[4] and is major cause for the functional impairment of actin filaments.[5]

In the course of oxidative stress, Met is first oxidized to its sulfur radical cation, which can subsequently complex with oxygen-, nitrogen-,or other sulfur-containing groups depending on the local arrangement. These groups act as Lewis bases by providing electron lone pairs leading to two-center three-electron (2c-3e) bonds,[6] designated as S∴X (X = N, O, or S), in which two electrons occupy the bonding $\sigma_{SX}$ orbital, the third one the $\sigma_{SX}^*$ antibonding one. This complexation increases the lifetime of the free radical, modifies its reduction potential and hence its reactivity, and determines the geometry of the final sulfoxide, which will in turn render possible or not the regeneration by the enzymatic systems.

Several studies were devoted to the experimental or theoretical characterization of the resulting S∴X bonds in peptides or in small model compounds (for review see ref 7 and references therein). Experimental data came mostly from pulse radiolysis and flash photolysis experiments in which the S∴X radicals were visualized by their absorption spectra. Hypotheses on the nature of the complexing groups and attribution of absorption spectra to each species were thus proposed,[8−10] which led to the following attribution of absorption wavelengths: 390 nm (SO radical cations), 450−520 nm (SS radical cations). As for SN radicals, experimental data seem to concern only deprotonated radicals. Regarding theoretical approaches they aimed at examining the stability of the conformers that might favor S∴X bonds in amyloid peptide,[11] Met[12] and *N*-acetyl-methioninamide,[13] Met Gly,[14] in cyclo-Met Met[15] and in organic compounds[16] and at predicting the wavelengths associated to the $\sigma \rightarrow \sigma^*$ absorption. The corresponding results are summarized in Table 1 for $S\therefore S^+$, $S\therefore N^+$, and $S\therefore O^+$ radical cations with the methods that were used in the different works. All the theoretical studies used DFT methods to investigate the structure, energetic, spectroscopic, and thermodynamic properties of the 2c-3e bonded species. However, none of them focused on the nature of the S∴X chemical bond, which could condition the redox properties of the radical intermediates and, hence, their reactivities.

Topological methods of chemical bonding aim to fulfill this goal, by "providing a mathematical bridge between chemical

* Corresponding author: Laboratoire de Chimie Théorique, Université Pierre et Marie Curie, 4 place Jussieu, boîte courrier 137, 75252 Paris cedex 5, France, fourre@lct.jussieu.fr.

† Université Pierre et Marie Curie, UMR 7616, Laboratoire de Chimie Théorique.

‡ CNRS, UMR 7616, Laboratoire de Chimie Théorique.

§ Université Paris Descartes.

|| Université Paris Sud, UMR 8000, Laboratoire de Chimie Physique.

10.1021/jp911983a 
Published on Web 06/17/2010

**TABLE 1: Compilation of Theoretical Results Obtained Previously on S∴X$^+$ Cyclic Radical Cations, X = S, N, or O[a]**

| Entry | Radical type | Compound | $R_{SX}$ | λ | f |
|---|---|---|---|---|---|
| 1 | SS | c(Met-Met)$^{+\cdot}$ | 3.04<br>*2.89* | 594[b]<br>*533*[b′] | 0.08[b]<br>*0.07*[b′] |
| 2 | SN5pep | 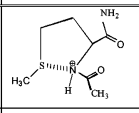 | 2.69 | *~475*[c] | |
| 3 | | 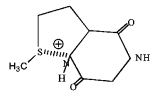 | 2.72<br>2.62[b″]<br>*2.81* | 485[b]<br>*429*[b′]<br>*356*[b′] | 0.13[b]<br>*0.02*[b′]<br>*0.02*[b′] |
| 4 | SN6pep | 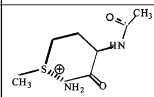 | 3.09[c′] | | |
| 5 | SO6carb | 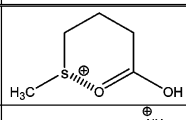 | 2.50<br>*2.41* | 428[d]<br>341[e]<br>*322*[e′] | 0.11[d] |
| 6 | | 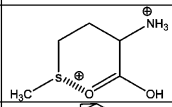 | 2.72[f]<br>*2.39* | *380*[e′] | |
| 7 | | 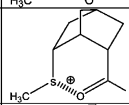 | 2.47<br>*2.37* | 431[d]<br>411[d]<br>*385*[e′] | 0.04[d]<br>0.04[d] |
| 8 | | 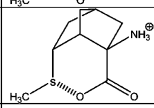 | *2.35* | *356*[e′] | |
| 9 | SO6pep | 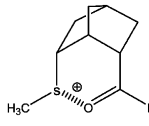 | 2.41<br>*2.41*<br>2.39<br>2.39 | 411[d]<br>321[e]<br>*322*[e′]<br>*408*[f]<br>*411*[f] | 0.12[d]<br>*0.15*[f]<br>*0.14*[f] |
| 10 | | 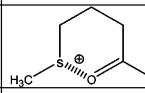 | 2.44<br>*2.43* | 427[d]<br>343[e]<br>*355*[e′] | 0.15[d] |
| 11 | | 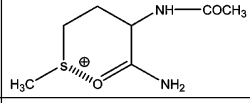 | 2.40[g]<br>2.41<br>*2.40* | 408[d]<br>333[e]<br>*321*[e′] | |
| 12 | | 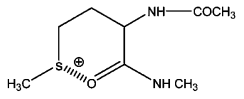 | 2.40<br>*2.41* | 416[d]<br>407[e]<br>*335*[e′] | *0.12*[e′] |
| 13 | SO7pep | 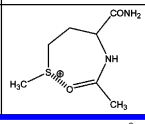 | 2.47[e′, g] | *450*[e] | |

[a] SX bond lengths ($R_{SX}$ in Å), absorption wavelengths (λ, in nm), oscillator strengths (f). In water the SO6carb species to be considered are the zwitterionic ones. Numbers in roman characters (respectively in italics) are calculated in vacuum (respectively in water). Calculation methods for the structural and spectroscopic parameters are indicated for each species; otherwise specified, the lowest level is that of the geometry optimization. [b] TD-B3LYP/6-311+G(d,p)//B3LYP/6-31G(d).[43] [b′] B3LYP(IEFPCM)/6-31G(d) for geometry optimization and TD-B3LYP(IEFPCM)/6-311+G(d,p)//B3LYP/6-31G(d) for spectroscopic parameters.[43] [b″] BH&HLYP/6-31G(d).[43] [c] TD-B3LYP(CPCM)/6-311+G(d,p)B3LYP/6-31G(d).[43] [c′] B3LYP/6-31G(d).[13] [d] TD-B3LYP/6-311+G(d)//B3LYP/6-311+G(d).[14] [e] ZINDO/S//B3LYP/6-311+G(d).[14] [e′] ZINDO/S//B3LYP(IEFPCM)/6-311+G(d).[14] [f] B3PW91/6-31+G(d).[16] Two conformational minima were found, with the same SO distance. [f] TD-B3PW91(IEFPCM)/6-31+G(d)//B3PW91/6-31+G(d).[16] [g] B3LYP/6-31G(d).[12]

intuition and quantum mechanics".[17] They require the knowledge of a scalar function of the space coordinates which carries the chemical information and relies on the theory of gradient dynamical systems.[18] This theory enables a partition of the molecular position space in adjacent regions of different nature and number, according to the chosen scalar function. Bader, who pioneered the use of topological concepts to analyze chemical systems in his atoms-in-molecules theory (AIM)[19] chose the electronic density. A chemical picture of the molecule made of atoms is thus recovered, but the partition does not explicitly reveal a substructure corresponding to the cores and the valence shell of the atoms. To overcome the conceptual limits of the topological analysis of the sole electron density, an alternative choice has been done by Silvi and Savin[20] and by Haüssermann et al.[21] who used the electron localization function (ELF) of Becke and Edgecombe.[22] The ELF, which can be viewed as a local measurement of the Pauli repulsion, is confined to the [1,0] interval, in order to tend to 1 where the Pauli repulsion is weak, i.e., in regions dominated by opposite spin pairs (or a lone electron) and to zero in regions dominated by the same spin pairs.[23] The partition of the molecular space that is obtained fulfills as well as possible a one-to-one correspondence with the Lewis representation of valence theory.[24,25]

The aim of the present work is several-fold: (i) to determine the various cyclic radical conformers resulting of the formation of S∴X intramolecular bonds and to re-examine the problem of their stability; (ii) to calculate their UV−visible absorption wavelengths; (iii) to characterize topologically these 2c-3e bonds as a function of the sequence. To fulfill this goal, we made a systematic study of the various species obtained after withdrawal of an electron from three peptides containing methionine, Met Gly, Gly Met, and Met Met (section III.A). The radical center was always localized on the sulfur atom, which, according to the conformation, could make an intramolecular 2c-3e bond with N, O, or another S. We considered the various possible numbers of atoms in the cycles (from 5 to 10) and optimized the corresponding structures in vacuum and in water, without searching all the stable conformers. For S∴O$^+$ and S∴N$^+$ complexes, we compared the different possibilities of 2c-3e bond formations: with an atom of the peptidic bond compared to that of the C- or N-terminal function. The absorption wavelengths and associated oscillator strengths were computed for each stable species (section III.B). Whenever it was possible, these results were compared to those concerning small intermolecularly S∴X$^+$ bonded models[26] and to those obtained by other theoretical studies concerning similar compounds (Table 1). We then performed a topological study of each radical cation using both AIM and ELF approaches (section III.C). From these structural, spectroscopic, and topological results, we extracted a new description of the 2c-3e bonding on methionine radical cations in dipeptides.

## II. Methodology

**A. Computational Methods.** From the methodological point of view, until now, the answer to which theoretical treatments are adequate for 2c-3e bonds is far from definitive. Single-reference configuration interaction methods such as QCISD(T) or CCSD(T) ones, with very large basis sets, lead to accurate energies and to reliable structures at the same time. However the sizes of the dipeptide radical cations investigated in this work were too large to perform energy optimizations with these methods. In addition, important discrepancies appeared between commonly used DFT methods.[27] Usually, the bond lengths and the binding energies are overestimated except with the BH&HLYP functional, leading to similar binding energies as CCSD(T) calculations for a set of small molecules.[26] We thus

privileged the BH&HLYP functional in the spin-unrestricted formalism and used the standard 6-31G(d) basis set. The use of this relatively small basis set is justified by the fact that DFT methods are not very basis-set dependent. All structures were fully optimized using the analytical gradient technique, and the nature of each located stationary point was checked by evaluating harmonic frequencies. Solvation effects were accounted for the corresponding zwitterionic compounds with the COSMO option for the polarized continuum model CPCM and their structures were fully reoptimized. Time-dependent density functional theory with BH&HLYP was used to calculate the UV−visible transitions of the S∴X bonds, which can remain a good compromise. The more sophisticated MRCI+Q method can hardly be used for these systems, but we used it for smaller models[26] and we have shown that the transition energy is less than 0.5 eV (the maximum error reported for the TD-DFT method[28]). We have checked the influence of the basis set (cc-pVTZ and 6-311+G(d,p)) for the radicals in vacuum and concluded that it was minor so we chose the 6-311+G(d,p) one to calculate the wavelengths of the solvated species. Calculations were performed with the Gaussian03 package.[29]

**B. Topological Signatures of the 2c-3e Bond.** Numerous papers have been dealing with the study of chemical bonding in molecules and solids, of reactivity, and of chemical reactions in the framework of the topological analysis of ELF (see ref 30 and references therein, in particular[31] for the theoretical foundations) or in the framework of the AIM theory.[32,33] Thus these two approaches will not be detailed here. From our preceding studies,[30,34−36] four ELF topological signatures have been established for the 2c-3e X∴Y bonding. In a recent work[26] we deduced three AIM signatures from the ELF ones. They provide a more global description of 2c-3e bonded complexes (due to the partition of the molecular space in atomic basins rather than in core and valence ones in the ELF approach) and should be examined first. These AIM and ELF criteria are defined in greater detail in Supporting Information and will be only briefly recalled below:

***AIM Topological Signatures of a 2c-3e X∴Y Bond.*** (1) As expected for an unshared-electron interaction, at the bond critical point located along the bond path linking the X and Y atoms, the gradient of the electron density vanishes, and its Laplacian is positive.[19,37]

(2) The lone electron being shared between the X and Y atoms, the corresponding integrated half-spin densities verify $\langle S_z\rangle_X + \langle S_z\rangle_Y \cong 0.5$, where $\langle S_z\rangle_{\Omega_i}$ is defined by

$$\langle S_z\rangle_{\Omega_i} = \frac{1}{2}\int_{\Omega_i} (\rho^{\alpha}(r) - \rho^{\beta}(r))\, \mathrm{d}r$$

Strongest 2c-3e bonds are characterized by well-balanced sharing of $\langle S_z\rangle$ between the two atomic basins.

(3) The electron fluctuation that occurs between the two atoms can be topologically quantified by a delocalization index $\delta_{X,Y}$, first defined by Fradera et al.[38] This index is maximal for homonuclear bonds and decreases as the difference in electronegativity of the fragments increases.

***ELF Topological Signatures of a 2c-3e X∴Y Bond.*** In the ELF approach, there is no more bond paths, but core basins and valence basins. The first ELF signature specifies the latter ones: "there is no $V$(X,Y) disynaptic basin associated with a 2c-3e X∴Y bond. Nevertheless the monosynaptic basins $V$(X) and $V$(Y) share a common separatrix". The second and third signatures defined in the AIM approach still stand, but the X and Y atomic basins should be replaced by the $V$(X) and $V$(Y) monosynaptic ones. Finally, using the reduction of the localization domain tree-diagram,[38] it is possible to introduce a core−valence bifurcation (CVB) index, similarly as the one successfully introduced by Fuster et al. to discriminate between weak and medium H-bonds.[39] Our CVB index is positive (respectively negative) for a 2c-3e bond (respectively for a mainly electrostatic interaction).[26,34,36]

## III. Results

In this work we focused on some conformations of the radical cations of three dipeptides, Gly Met, Met Gly, and Met Met that can make intramolecular S∴X bonds (X = S, N, O). We adopted the following nomenclature: for the S∴$N^+$ radicals, S can be linked either to N of the amine function (SNam) or to N of the peptidic bond (SNpep). Also, the number of atoms in the pseudocycle is included in the nomenclature (for instance SN5 for five atoms). For the SN5pep compounds we investigated two conformations (SN5pep1 and SN5pep2) corresponding to noticeably different SN distances. Similar nomenclature was used for S∴$O^+$ radicals: SOcarb (respectively SOcarbH) refers to a bond with the divalent oxygen (respectively with the protonated oxygen) of the carboxylic group, SOpep to the carbonyl of the peptidic bond. Our structural and spectroscopic results were compared, whenever possible, to those obtained by other authors on similar compounds and summarized in Table 1. One must keep in mind that some of the discrepancies might arise from differences in methodology, particularly for spectroscopic results. Their structures were usually optimized using B3LYP functional and eventually IEFPCM model for solvation, which explained that their SX bond lengths were usually larger than ours. Their absorption wavelengths were calculated using ZINDO/S or TD-B3LYP methods and substantial differences may arise even for similar SX distances.

**A. Structures and Energies.** The fully optimized geometries of the selected radical cations are shown in Figure 1. For each S∴$X^+$ radical under scrutiny, absolute energies, as well as the SX bond length, the absorption wavelength, and the corresponding oscillator strength, calculated in vacuum and in water are reported in Table 2. The energies of the various cations as a function of the SX distance are displayed in Figure 2.

***S∴S$^+$ Radical Cations.*** When X = S, the stabilization due to the formation of the 2c-3e S∴X bond is maximum;[41] thus homonuclear-like S∴$S^+$ radicals were the starting point of our study. Since we looked only for intramolecular bonds, the parent peptide was Met Met. For the conformer displayed in Figure 1 the SS bond length is 2.96 Å in vacuum, which can be compared to several intermolecular SS 2c-3e bond lengths: in $Me_2S\therefore SMe_2^+$ (Me = $CH_3$), using the same method and basis we found an optimized bond length of 2.84 Å, significantly shorter than in the dipeptide. The B3LYP study of Bergès et al.[42] pointed out the influence of the size and nature of the substituent. Indeed the SS distance increases from $R_{SS}$ = 2.79 Å for $Me_2S\therefore SMe_2^+$ up to $R_{SS}$ = 2.94 Å for diSETAc cation ($C_2H_5(CH_3{-}CO){-}S\therefore S{-}(CO{-}CH_3)C_2H_5^+$), and to $R_{SS}$ = 3.01 Å for the diSETA cation ($C_2H_5(CH_3{-}CO)CH_2{-}S\therefore SCH_2{-}(CO{-}CH_3)C_2H_5$). Hence the rather large value obtained in the Met Met cation could result not only from the geometrical constraints but also from the substituent effects.

In water, the structure is almost unchanged, except for the formation of a H-bond (see Figure 1), and the SS bond length increases by 0.07 Å.

For c-(Met Met) (entry 1 of Table 1), Bobrowski et al. obtained $R_{SS}$ = 3.04 Å.[43] Not only the parent dipeptide is not

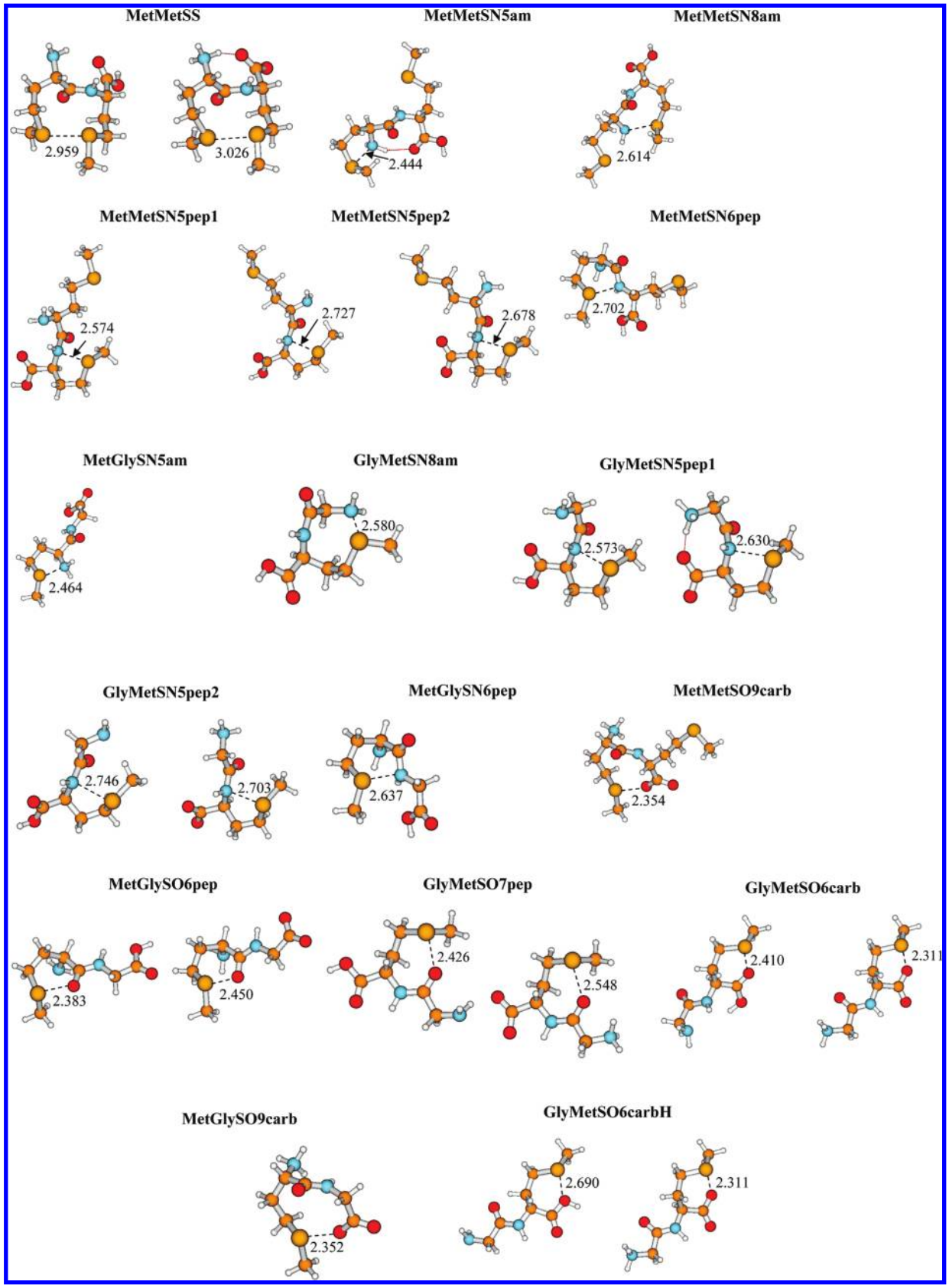


**Figure 1.** The optimized geometries of the radical cations in vacuum (left) and in water (right, when available). Distances are in angstroms.

the same as MetMetSS ($R_{SS}$ = 2.96 Å), the cyclization inducing a supplementary constraint, but this greater value may also be due to their use of the B3LYP functional. In their solvated compound no H-bond occurs and the SS distance decreases by 0.15 Å. Though our solvation model is not the same, the lengthening of the SS bond in MetMetSS ($R_{SS}$ = 3.02 Å) could originate from the competitive formation of one H-bond.

***S∴N*$^+$ *Radical Cations.*** In vacuum, among the SN radicals, stable five-membered cycles were found with the three peptides. In Gly Met only the peptidic bond could be involved, in Met

**TABLE 2: Structure and Spectroscopy of the S∴X$^+$ Species with X = S, N, and O[a]**

| compound | *E* | $R_{SX}$ | $\lambda$ | *f* |
|---|---|---|---|---|
| MetMetSS | −1523.944934 | 2.96 | 642 | 0.20 |
| | *−1524.026059* | *3.02* | *719* | *0.16* |
| MetMetSN5am | −1523.959161 | 2.44 | 345 | 0.19 |
| MetGlySN5am | −1007.921145 | 2.46 | 348 | 0.23 |
| MetMetSN8am | −1523.951034 | 2.61 | 479 | 0.11 |
| GlyMetSN8am | −1007.898137 | 2.58 | 422 | 0.14 |
| MetMetSN5pep1 | −1523.947020 | 2.57 | 419 | 0.16 |
| GlyMetSN5pep1 | −1007.915451 | 2.57 | 415 | 0.17 |
| | *−1008.001381* | *2.63* | *475* | *0.16* |
| MetMetSN5pep2 | −1523.942240 | 2.73 | 481 | 0.09 |
| | *−1524.026541* | *2.68* | *520* | *0.15* |
| GlyMetSN5pep2 | −1007.910214 | 2.75 | 475 | 0.07 |
| | *−1007.992550* | *2.70* | *518* | *0.15* |
| MetMetSN6pep | −1523.919174 | 2.70 | 550 | 0.19 |
| MetGlySN6pep | −1007.888191 | 2.64 | 478 | 0.17 |
| MetGlySO6pep | −1007.915380 | 2.38 | 359 | 0.11 |
| | *−1007.989031* | *2.45* | *380* | *0.14* |
| | | | *407* | *0.04* |
| GlyMetSO7pep | −1007.909539 | 2.43 | 396 | 0.06 |
| | *−1008.000099* | *2.55* | *319* | *0.04* |
| | | | *343* | *0.07* |
| GlyMetSO6carb | −1007.906571 | 2.41 | 298 | 0.04 |
| | *−1008.014333* | *2.31* | *371* | *0.21* |
| GlyMetSO6carbH | −1007.889201 | 2.69 | 286 | 0.03 |
| | *−1008.014333* | *2.31* | *371* | *0.21* |
| MetMetSO9carb | *−1524.029389* | *2.35* | *427* | *0.19* |
| MetGlySO9carb | *−1007.996082* | *2.35* | *421* | *0.17* |

[a] Absolute energies (*E*, in hartrees) and SX distances ($R_{SX}$, in Å) of the optimized compounds, obtained at the BH&HLYP/6-31G(d) level in vacuum (roman characters) and at the BH&HLYP(CPCM)/6-31G* level in water (italics characters); absorption wavelengths ($\lambda$, in nm) and oscillator strengths (*f*) calculated at the TD-BH&HLYP/6-311+G(d,p)// BH&HLYP/6-31G(d) level in vacuum (roman characters) and at the TD-BH&HLYP(CPCM)/6-311+G(d,p)// BH&HLYP(CPCM)/6-31G(d) level in water (italics characters).

Gly only the amine function made a bond with the S atom, whereas in Met Met the two types of bonds were found, SN5pep and SN5am (Figure 1). In all peptides, among SN5 radical cations the energy increased with the SN bond lengths (Figure 2A and 2C). The SN distance was shorter in the SN5am radicals (around 2.45 Å) than in SN5pep1 (2.57 Å). This trend was more pronounced in the corresponding intermolecularly bonded SN radicals, $Me_2S∴NH_2Me^+$ (SNam type, 2.52 Å) and $Me_2S∴NHMeCOH^+$ (SNpep type, 2.77 Å),[25] maybe due to the lack of cyclization constraints. In SN5pep2 radicals the nitrogen of the amine group pointed toward the hydrogen of a methyl group, leading to a SN distance noticeably greater than in SN5pep1 (around 2.74 Å). The steric hindrance between the amine and the methyl could be at the origin of the longer SN distance in these species. The SN5am radicals are the most stable structures, compared to SN5pep (Figure 2A and 2C). The topological analysis will enlighten the structural differences between SN5am and SN5pep radicals (vide infra). The SN6 cyclic radicals that were found, MetMetSN6pep and MetGlySN6pep, had similar behaviors: (i) larger SN distances (2.70 and 2.64 Å) than in SN5pep1, as expected for larger cycles, and (ii) relatively high energies in the series (25 and 21 kcal·mol$^{-1}$ higher than the SN5am radicals, as shown in Figure 2C and 2A). Finally SN8 cycles were obtained with Met Met and Gly Met and involve the amine function. The SN bond distance was also longer (by about 0.15 Å) than those of SN5am compounds. Both radicals are higher in energy than the isoelectronic SN5am compounds, by 5 kcal.mol$^{-1}$ for MetMetSN8am and 14 kcal.mol$^{-1}$ for GlyMetSN8am.

In water, only the zwitterions of MetMetSN5pep2, GlyMetSN5pep1, and GlyMetSN5pep2 are stable. Generally, the geometries of the cyclic structures remain roughly close but

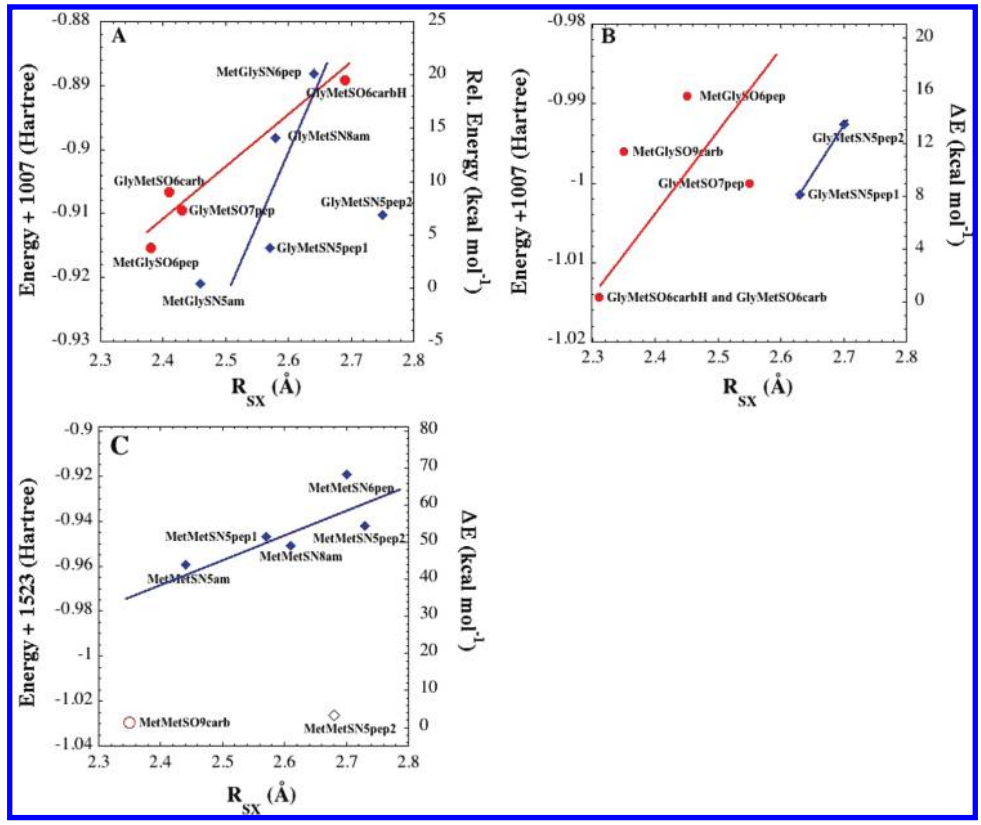


**Figure 2.** Energies of the radical cations as a function of the SX distance: (A) Met Gly and Gly Met in vacuum; (B) Met Gly and Gly Met in water; (C) Met Met in vacuum and in water. red circle, SO radicals; blue diamond shape, SN radicals. (C) blue diamond shape, SN radicals in vacuum; red open circle, blue open diamond shape: SO and SN in water, respectively. The straight lines are visual fits.

not identical to those in vacuum. The SN bond lengths decrease by about 0.05 Å, except for GlyMetSN5pep1 in which it increases by 0.06 Å, probably because of the formation of a H-bond between the $NH_3^+$ and the $COO^-$ groups. As for both SN6pep compounds, no corresponding SN6 zwitterions could be obtained.

Intramolecular SNpep type structures were also described by other authors following oxidation of *N*-acetylmethioninamide[13] (entries 2 and 4 of Table 1) or of c-(Met Gly) (entry 3 of Table 1). For SN5pep the bond lengths in vacuum are around 2.7 Å (entries 2 and 3), larger than in our SN5pep1 compounds (2.57 Å), maybe due to the use of B3LYP. It can be noticed that when entry 3 was optimized at the BH&HLYP/6-31G(d) level, a SN distance of 2.62 Å was obtained,[43] in close agreement with our results. In water, its equilibrium distance is 2.81 Å, whereas ours are in the range 2.6−2.7 Å. A stable structure was found by Brunelle et al.[13] for a SN6pep type compound, but its bond length is very large (3.09 Å, entry 4, Table 1) compared to our values (∼2.7 Å) corresponding to a rather loose 2c-3e interaction.

***S∴O⁺ Radical Cations.*** SO radical cations were found in Met Gly, Gly Met. In MetMet it was found in water only (in vacuum it evolved toward a SN one). Cycles involving six, seven, or nine atoms were obtained (the nine atoms cycle only in water). In vacuum, for the SOpep and SOcarb radical cations, the SO distances are close to 2.4 Å, GlyMetSO6carb being slightly longer than MetGlySO6pep by 0.03 Å. This lengthening was more pronounced for the corresponding intermolecularly bonded SOpep type radical, $Me_2S\therefore OCMeNH_2^+$ and SOcarb one, $Me_2S\therefore OCMeOH^+$ (SO bond length increasing from 2.41 to 2.50 Å). In GlyMetSO6carbH, the SO distance is much longer (2.69 Å) than those of SOpep or SOcarb, indicating a weaker S···O interaction. Indeed the stability of the SOcarb compound is comparable to that of the SOpep ones (within a range of 5 kcal/mol), far from the SO6carbH radical ($\Delta E = 16.4$ kcal/mol with respect to the most stable MetGlySO6pep, Figure 2A). Assuming that the bonding properties of the $\sigma_{SO}$ plays a crucial role in the relative stability of the SO radicals, it is worthy to note that the contribution of the oxygen p lone pair decreases from MetGlySO6pep and GlyMetSO7pep to GlyMetSO6carb and then to GlyMetSO6carbH (about 33% in MetGlySOpep and only 20% in GlyMetSO6carbH), as the relative energies increase.

Upon solvation, conversely to the SNpep radicals, the SO distances in SOpep radicals increased (by 0.07−0.12 Å) whereas in GlyMetSO6carb the SO bond shortened by 0.10 Å. Interestingly GlyMetSO6carbH leads to the same zwitterionic structure as GlyMetSO6carb. In this zwitterion, the oxygen is negative and the sulfur positively charged, leading to a neutral S···O bond noticeably shorter than a S···O⁺ one (this shortening of the SO distance had already been noted for $(CH_3)_2S\therefore OH$).[36] Compared to the results obtained in vacuum, the order of stabilities between the previous SOcarb and SOpep compounds is reversed (Figure 2B). This is consistent with the bond shortening in SOcarb species (vide supra). A neutral interaction is also observed for MetMetSO9carb and MetGlySO9carb, with a similar short SO bond (2.35 Å). These SO9carb cycles appeared only in water and originate from the solvation of the SN6pep species.

Conversely to the SN compounds a comparatively large amount of theoretical studies were devoted to SO type radicals (entries 5−13 of Table 1). For SO6carb compounds, the decrease of the SO bond length by 0.1 Å that we obtained from vacuum to water is also reproduced by other authors (entries 5 and 7, Table 1), although the absolute values are ∼0.1 Å greater than ours. For SO6pep radicals (entries 9−12, Table 1) equilibrium distances in vacuum as well as in water are always close to 2.4 Å, in good agreement with our results for MetGlySO6pep. Finally, one SO7pep radical was investigated by Brunelle et al.,[12] they obtained $R_{SO} = 2.47$ Å in vacuum (entry 13, Table 1), in very good agreement with our value for GlyMetSO7pep.

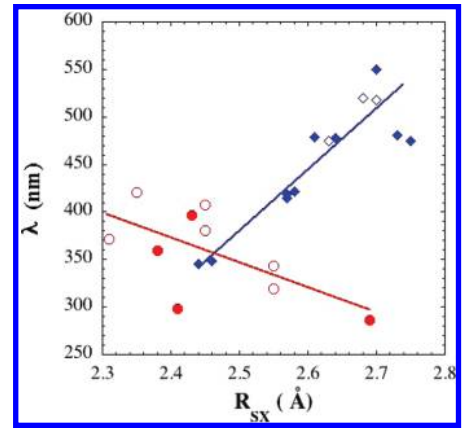


**Figure 3.** Absorption wavelength associated to the $\sigma \rightarrow \sigma^*$ transition as a function of the SX distances: solid and open diamond shape, S∴N⁺ radical cations; solid and open circles, S∴O⁺ radical cations; filled symbols, in vacuum; open symbols, in water.

Comparing the SN and SO radicals it can be noticed that several compounds had quasi-equal absolute energies: in vacuum, GlyMetSN5pep1 and MetGlySO6pep, GlyMetSN5pep2 and GlyMetSO7pep; and in water, GlyMetSN5pep1 and GlyMetSO7pep. This may be due to electronic factors, because in these cases the SO bond lengths are shorter than the SN ones.

Among the 17 structures that we have explored, Figure 2 shows that in vacuum the energy of the entities tend to increase with the SX bond length except for the SN5pep2. It means that a parameter for the stability of the radical cation could be the overlap of the p lone pairs of the two heteroatoms involved in the 2c-3e bond. Also in vacuum, the most stable cycles are made of five atoms. They involve nitrogen and exhibit short SN bonds (ca. 2.45 Å).

In water only seven optimized structures could be characterized. However, for Gly Met we obtained several structures in water, and the most stable ones had a SO bond with the carboxylic/carboxylate group.

**B. Absorption Wavelengths.** The absorption wavelengths and oscillator strengths of all radicals, in vacuum and in water, are gathered in Table 2. The $\lambda$ values vary from 286 nm (GlyMetSO6carbH) to 642 nm (MetMetSS) in vacuum and from 319 nm (GlyMetSO7pep) to 719 nm (MetMetSS) in water. This large range of variation is rationalized by reporting them as a function of the SX bond length ($R_{SX}$, X = N, O) in vacuum as well as in water (Figure 3). There are two opposite trends: $\lambda$ increases quasi-linearly with $R_{SX}$ for the SN radicals whereas it decreases for the SO ones (albeit with a lower correlation factor). For SN entities $\lambda$ varies from ∼345 nm ($R_{SN}$∼2.45 Å in the most stable SN5am (vide supra), $f \sim 0.20$), to the largest value 550 nm ($R_{SN} = 2.70$ Å for MetMetSN6pep, $f = 0.19$). For the SO radicals, the $\lambda$ values vary from 286 nm ($R_{SO} = 2.69$ Å, GlyMetSO6carbH) to ∼425 nm ($R_{SO} = 2.35$ Å, SO9carb compounds). The increase of $\lambda_{SN}$ as a function of $R_{SN}$ is consistent with the 2c-3e nature of the SN bond: indeed the corresponding decrease of the $\sigma/\sigma^*$ gap is expected as the overlap of the S and N lone pairs decreases. Conversely the decrease of $\lambda_{SO}$ confirmed that the S···O bond is of different nature, mainly electrostatic (see the topological analysis).

In our previous work on small intermolecularly bonded S∴S$^+$, S∴N$^+$, and S∴O$^+$ radicals cations[25] the $\lambda$ values were very close to those obtained for the corresponding dipeptide radical cations (481 nm for S∴N and 412 nm for S∴O against 428 nm for MetGlySN6pep and 396 nm for GlyMetSO7pep) whereas for the S∴S$^+$ radical the larger difference between inter- and intramolecularly bonded compounds (596 nm compared to 642 nm) suggested that the effect of cyclization was more important.

***Comparison with Other Theoretical Studies.*** For the SS radical cations, in agreement with the discrepancies between the structures of c-(Met Met)$^+$ and MetMetSS, great differences are observed between their absorption wavelengths in vacuum as well as in water: ∼590 and 530 nm for the former (entry 1, Table 1), 640 and 720 nm for the latter.

For SN radical cations absorption wavelengths are available only for SN5pep ones. In vacuum, $\lambda$ = 485 nm for entry 3 of Table 1, at the upper border of our range of 420−480 nm, and in water two values were reported $\lambda$ ∼430 and 360 nm, far below our results (475−520 nm) but with negligible oscillator strengths. For entry 2 the reported $\lambda$ value, which was calculated in water with the vacuum geometry ($R_{SN}$ ∼ 2.7 Å), fits very well with that of GlyMetSN5pep1 (475 nm, $R_{SN}$ ∼ 2.6 Å).

For SO6 compounds (entries 5−12), the available wavelengths were calculated with either TD-DFT and (or) ZINDO/S approaches. The ZINDO/S $\lambda$ values are shifted by 75−90 nm toward the UV region with respect to the TD-DFT ones, falling in the 320−340 nm range (in vacuum as well as in water, except for entry 12). They will not be discussed except if TD-DFT values are not available. For SO6carb compounds wavelengths in vacuum (entries 5 and 7, Table 1) are greater than ours (410−430 nm against ∼300 nm). In water, the only available $\lambda$ values are ZINDO/S ones. Nevertheless, the agreement is better than in vacuum (320−385 nm for entries 5−8 against 371 nm for GlyMetSO6carb). The TD-DFT absorption wavelengths of SO6pep radicals in vacuum (entries 9−12, Table 1) are in the region 410−430 nm, with $R_{SO}$ values always around 2.4 Å. The lower border is 50 nm greater than our value for MetGlySO6pep (∼360 nm). In water, some TD-DFT values exist for entry 9, with significant oscillator strengths around 410 nm. For MetGlySO6pep radical we obtained a non-negligible oscillator strength at 380 nm, which agrees rather well with these results. Finally, for SO7pep radicals, there is a large discrepancy between the $\lambda$ value reported in water for entry 13 of Table 1 (450 nm) and that of GlyMetSO7pep (319 nm). However, it is noteworthy that the geometry of the former radical was not reoptimized in the solvent, which may explain why the agreement is better if the comparison is done with the value we obtained in vacuum (396 nm).

**C. Topological Analysis.** Table 3 gives the AIM topological parameters of selected compounds in vacuum (one of each type). For all of them the first AIM signature of the 2c-3e bond is verified; i.e,. the electronic density at the bond critical point (BCP) is low (0.2−0.3 e.Å$^{-3}$) and its Laplacian is positive, as in closed-shell interactions[19,36] (note that, except for MetMetSS, the relative position of the BCP with respect to S is remarkably constant). Moreover, the data clearly show that the lone electron remains almost entirely localized on the two heteroatoms involved in the 2c-3e S∴X bond: indeed the sum of the S and X contributions to the integrated half-spin density $\langle S_z \rangle$ is always greater than 0.45. The best sharing of $\langle S_z \rangle$ is evidently obtained for MetMetSS, but contrary to homodimeric internuclear 2c-3e complexes, the two values of $\langle S_z \rangle$ are not strictly equal, since the two sulfur atoms have slightly different environments. We note that the spin polarization ($2 \times \langle S_z \rangle$) of the sulfur atom increases in the series X = S, N, O, and hence the delocalization of the lone electron (roughly) decreases, as the electronegativity of the X atom increases: for example 42% of the spin is on S (of the N-terminal Met) with $\delta_{SS}$ = 0.50 in MetMetSS, 58% in MetMetSN8am with $\delta_{SN}$ = 0.46, whereas this proportion reaches 76% in MetGlySO6pep, with $\delta_{SO}$ = 0.40. These variations are in agreement with the second and third AIM signatures of 2c-3e bonds. Looking in more detail, $2 \times \langle S_z \rangle_S$ is a bit larger (0.64 against ∼0.60) and $\delta_{SN}$ is smaller (∼0.40 against ∼0.50) in SNpep than in SNam. Similarly $2 \times \langle S_z \rangle_S$ is slightly larger (0.80 against ∼0.76) and $\delta_{SO}$ is smaller (0.34 against ∼0.40) in SOcarb than in SOpep. This indicates that an amino nitrogen (a peptidic oxygen) is more donating than a peptidic nitrogen (a carboxylic oxygen), as expected from the highest localization of the lone pair of the peptidic nitrogen (of the carboxylic oxygen). For a given S∴X bond, $\delta$ also decreases by increasing the bond distance (0.50 and $R_{SN}$ = 2.41 Å for MetMetSN5am, against 0.46 and $R_{SN}$ = 2.61 Å in MetMetSN8am). All these trends agree well with the ones obtained previously for the small models of 2c-3e radical cations of dipeptides.[25] The surprisingly low $\delta_{S,S}$ value that is obtained for MetMetSS (equal to that of MetMetSN5am) can be explained by the very large value of $R_{SS}$, compared to that of $R_{SN}$.

In the ELF topological approach, the valence basins implied in the 2c-3e bonds can be specified. For all compounds considered in this paper the first ELF signature of a 2c-3e S∴X bond is verified, as illustrated in Figure 4 for three representative radical cations: indeed no disynaptic basin $V$(S,X) was found, and the two monosynaptic basins $V$(S) and $V$(X) share a common separatrix. Table 4 gives the quantitative ELF parameters for all the compounds investigated, in vacuum as in water,

**TABLE 3: AIM Topological Parameters for the Heteroatoms Involved in the Intramolecular S∴X Bond (X = S, N, O), for One Radical of Each Type, in Vacuum: S∴X Bond Critical Point (BCP) Properties ($R_S/R_{SX}$, $\rho_b$, $\nabla^2\rho_b$)[a], Integrated Half-Spin Densities of the Atomic Basins, $\langle S_z \rangle$, and Delocalization Index, $\delta_{S,X}$, between These Basins**

| compound | $R_S/R_{SX}$ | $\rho_b$ | $\nabla^2\rho_b$ | $\langle S_z \rangle_S$ | $\langle S_z \rangle_X$ | $\delta_{S,X}$ |
|---|---|---|---|---|---|---|
| MetMetSS[b] | 0.497 | 0.199 | 1.436 | 0.21 | 0.25 | 0.50 |
| MetMetSN5am | 0.520 | 0.343 | 2.482 | 0.30 | 0.17 | 0.50 |
| MetMetSN8am | 0.525 | 0.256 | 1.938 | 0.29 | 0.17 | 0.46 |
| MetMetSN5pep1 | 0.525 | 0.266 | 2.003 | 0.32 | 0.13 | 0.40 |
| MetMetSN6pep | 0.526 | 0.216 | 1.685 | 0.32 | 0.14 | 0.38 |
| MetGlySO6pep | 0.525 | 0.312 | 3.068 | 0.38 | 0.10 | 0.40 |
| GlyMetSO7pep | 0.527 | 0.281 | 2.844 | 0.37 | 0.10 | 0.38 |
| GlyMetSO6carb | 0.523 | 0.285 | 2.928 | 0.40 | 0.07 | 0.34 |

[a] $R_s$ = distance between atom S and the bond critical point, in Å; $\rho_b$ is the electronic density at the BCP, in e.Å$^{-3}$ and $\nabla^2\rho_b$ the Laplacian of $\rho$ at this point, in e•Å$^{-5}$. [b] For this radical S = $S_1$ (N-terminal Met) and X = $S_2$ (C-terminal Met) (see Figure 4).

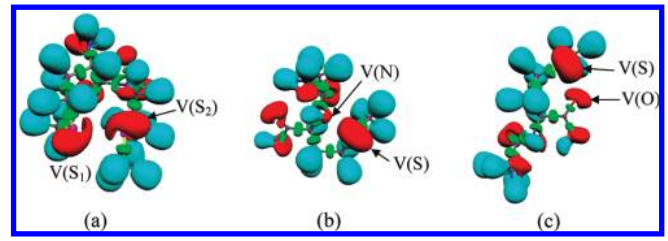


**Figure 4.** ELF = 0.8 isosurfaces of three representative radical cations: (a) MetMetSS, (b) GlyMetSN5pep1, and (c) GlyMetSO6carb. The localization domains corresponding to the monosynaptic basins of the heteroatoms involved in the S∴X bond are indicated by $V$(S) and $V$(X), with X = S, N, O.

**TABLE 4: ELF Topological Parameters for the Heteroatoms Involved in the Intramolecular S∴X Bond (X = S, N, O): Integrated Half-Spin Densities of the Monosynaptic Basins, $\langle S_z \rangle$, Delocalization Index $\delta_{V(S),V(X)}$ between These Basins, and Core Valence Bifurcation Index, $\theta$(3e) (positive ones in bold)[a]**

| compound | $\langle S_z \rangle_{V(S)}$ | $\langle S_z \rangle_{V(X)}$ | $\delta_{V(S),V(X)}$ | $\theta$(3e) |
|---|---|---|---|---|
| MetMetSS | 0.17 | 0.19 | 0.38 | **0.00** |
| | *0.13* | *0.22* | *0.34* | *−0.03* |
| MetMetSN5am | 0.24 | 0.08 | 0.26 | **0.11** |
| MetGlySN5am | 0.23 | 0.09 | 0.26 | **0.09** |
| MetMetSN8am | 0.22 | 0.08 | 0.24 | **0.05** |
| GlyMetSN8am | 0.24 | 0.08 | 0.26 | **0.06** |
| MetMetSN5pep1 | 0.24 | 0.06 | 0.20 | **0.05** |
| GlyMetSN5pep1 | 0.24 | 0.06 | 0.20 | **0.04** |
| | *0.26* | *0.04* | *0.16* | *−0.03* |
| MetMetSN5pep2 | 0.27 | 0.04 | 0.14 | −0.03 |
| | *0.26* | *0.04* | *0.14* | ***0.00*** |
| GlyMetSN5pep2 | 0.28 | 0.03 | 0.14 | −0.05 |
| | *0.26* | *0.03* | *0.14* | *−0.03* |
| MetMetSN6pep | 0.24 | 0.06 | 0.18 | **0.01** |
| MetGlySN6pep | 0.25 | 0.06 | 0.20 | **0.02** |
| MetGlySO6pep | 0.28 | 0.08 | 0.26 | **0.03** |
| | *0.29* | *0.07* | *0.20* | *−0.05* |
| GlyMetSO7pep | 0.27 | 0.08 | 0.28 | −0.02 |
| | *0.30* | *0.05* | *0.18* | *−0.07* |
| | | | | *−0.09* |
| GlyMetSO6carb | 0.29 | 0.06 | 0.22 | −0.03 |
| | *0.25* | *0.11* | *0.34* | ***0.05*** |
| MetMetSO9carb | *0.21* | *0.16* | *0.40* | ***0.05*** |
| MetGlySO9carb | *0.22* | *0.15* | *0.38* | ***0.04*** |
| GlyMetSO6carbH | 0.31 | 0.02 | 0.10 | −0.13 |

[a] Numbers in roman (in italics) are the topological parameters in vacuum (in water). For this radical S = $S_1$ (N-terminal Met) and X = $S_2$ (C-terminal Met) (see Figure 4).

when available. The data allow specifying the localization of the lone electron, mainly into *V*(S) and *V*(X). The sum of the integrated basin half spin densities (∼0.36 for MetMetSS and S∴$O^+$ radicals, ∼0.30 for S∴$N^+$ radicals) is very similar to what was found previously for corresponding small models (see Table 3 of ref 26). When considering, in vacuum, the monosynaptic basins instead of the atomic ones, the trends previously extracted from the AIM approach, along the series S → N → O still stand, though generally less striking (signatures 2 and 3). They agree with the Pauling description of the S∴X bond in terms of resonating structures $S^{\bullet+}$ |X ↔ S| $^{\bullet+}$X and confirm the increasing contribution of $S^{\bullet+}$ |X as X goes from S to N to O (and also in a minor way as X changes from N-amino to N-peptidic and from O-peptidic to O-carboxylic). However, conversely to the AIM results, the $\langle S_z \rangle_{V(S)}$ values for SNam, SN5pep1, and SN6pep compounds remain constant (∼0.24) whereas the delocalization index markedly decreases (from 0.26 to 0.18). The spin polarization of *V*(S) in SN5pep2 radicals is greater and the delocalization index is lower than in SN5pep1 ones, due to larger $R_{SN}$. In SOpep and SOcarb, the ELF delocalization index is somehow larger (from 0.28 to 0.22) than expected from the value of $\langle S_z \rangle_{V(S)}$(∼0.28) (compared to SN compounds), maybe partly because the $R_{SO}$ bond lengths are smaller than $R_{SN}$ ones. The influence of the bond length in electron fluctuation can also be invoked in GlyMetSO6carbH, for which $\delta$ is very low compared to GlyMetSO6carb. The ELF description of the 2c-3e S∴X bond is achieved by examination of the core valence bifurcation index (CVB), $\theta$(3e), reported in the last column of Table 4. Surprisingly for MetMetSS, in which 2c-3e bonding is expected to be favored, this parameter is zero, maybe due to the very large SS distance (2.96 Å). In our previous study on model radical cations of dipeptides, we indeed observed a decrease of $\theta$(3e) from 0.09 to 0.01 on going from the optimized ($R_{SS}$ = 2.84 Å) to the constrained geometry (chosen to mimic the local conformation in the dipeptide, i.e., with $R_{SS}$ = 2.96 Å).

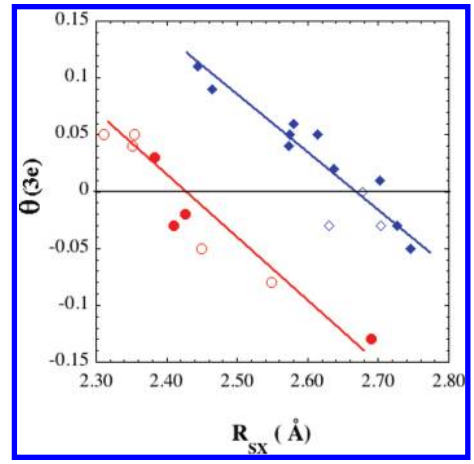


**Figure 5.** Variation of the core valence bifurcation index $\theta$(3e) of the S∴$X^+$ radical cations as a function of the SX distance (X = N or O): solid and open circles: SO radicals; solid and open diamond shapes, SN radicals; filled symbols, in vacuum; open symbols, in water. The straight lines are visual fits.

Figure 5 shows that for SN as well as for SO radicals, in vacuum as well as in water, $\theta$(3e) decreases by increasing $R_{SX}$. At constant distance, $\theta$(3e) is higher for SN than for SO radicals. Also, more SN radicals have $\theta$(3e) positive than SO, which indicates a higher 2c-3e character of the SX bond (vide infra). For most of the SN compounds in vacuum, $\theta$(3e) decreases from 0.11 to 0.01 along the series SN5am → SN8am → SN5pep1 → SN6pep thus indicating, together with the other ELF topological signatures, a weakening of the 2c-3e interaction. It is negative for SN5pep2 radicals (∼−0.05), signature of a mostly electrostatic interaction. Conversely to SN compounds, most of the CVB indexes of SO compounds in vacuum are negative. They decrease from −0.02 to −0.13 from GlyMetSO7pep and GlyMetSO6carb to GlyMetSO6carbH, except for MetGlySO6pep (0.03). Thus, from the whole ELF parameters, the S···O bond in radical cations of dipeptides in vacuum is generally best described as an electrostatic interaction. The modification of the nature of the intramolecular SX bond (X = S, O, N), from 2c-3e to electrostatic interaction, corroborates our previous findings for intermolecularly SX bonded model radical cations.[25]

Upon solvation the variations of the topological parameters and thus of the nature of the S∴X bond are also closely related to the variations of the bond length. Indeed, for SN5pep1 and SOpep compounds the delocalization index decreases with solvation in water (the largest variation is for GlyMetSO7pep, from 0.28 to 0.18) as the CVB index does (now negative in all cases). Both parameter variations mean a weakening of the 2c-3e character. For SN5pep2 and SOcarb radicals the inverse variations are obtained, thus indicating a strengthening of the 2c-3e character. In water, the zwitterionic nature of SOcarb (vide supra) renders the S∴O link neutral and the topological parameters show that the SOcarb radicals become 2c-3e bonded radicals.[36]

## IV. Conclusion

The structure of 2c-3e bonds involving sulfur has prompted a great number of studies by experiment as well as by quantum chemistry (see Table 1). These radicals not only present a

chemical interest but also appear to have biochemical and biological roles. Since theses entities are short-lived, their structures cannot be ascertained by experiment. Thus the contributions of optimizations by the methods of quantum chemistry are decisive. In polypeptides and proteins these sequences can be found either buried inside the macromolecules or in contact with the aqueous medium. Therefore to roughly mimic these environments, we have performed calculations in vacuum and in water.

We have considered three peptides with the residue Met in different relative positions, Met Gly, Gly Met, and Met Met, and we have selected 17 stable cyclic radical cations coming from these dipeptides, which differ by the SX intramolecular bonding. For each peptide, SN and SO bonds could be formed either with the peptidic bond or with the N- or C-terminal and the cycles could involve five to nine atoms. The most stable structures are SN5 cycles, and the energies increase almost linearly with the SX distances (Figure 2A and C) except for GlyMetSN5pep2, with different slopes for N and O.

In water, only seven zwitterionic compounds were obtained after full optimization from the 17 existing in vacuum and the most stable conformations are now the six-member rings with SO bond involving the carboxylate function (Figure 2B). Interestingly, for Met Met, the most stable conformation exhibits a larger nine-atom cycle.

As for the absorption wavelengths, Figure 3 shows that, in the SN radical cations they increase with the SN bond length in vacuum as well as in water, whereas in the SO compounds they slightly decrease by increasing the SO bond length. These different trends indicate deeper differences in the bond natures.

In order to understand why SN and SO compounds exhibit such different spectroscopic properties, we performed, for the first time to our knowledge, a topological study of the 2c-3e bonding in systems of biological interest. The AIM and ELF approaches confirmed that S∴N bonds are mainly of the 2c-3e type, the S∴S one in MetMetSS playing the role of prototype in this series of radical cations. The situation was more complex with S∴O bonds. Using the ELF formalism, we demonstrated that they were closer to electrostatic interactions (Figure 5). This finding allowed us to reinterpret the variation of absorption wavelengths with the bond length. Indeed, the molecular orbital description for 2c-3e bonds showed that the absorption wavelength associated to a $\sigma \rightarrow \sigma^*$ transition should increase with the bond length, whereas it roughly decreases for the SO radical cations (Figure 3). We have thus discovered that the different repartition of the electrons in the SN and SO bonds had important consequences on the absorption properties of the radical cations.

One should mention that in experimental studies of transients, the absorption spectra have great importance because very often they are the only way of observation and characterization of free radicals. As an example $S\therefore S^+$ radical cations were found to absorb around 500 nm (510 nm for the cyclic compound c(Met Met)$^{+}$ [9], 500 nm for the dimeric radical cation of SETA,[43] 480 nm for N-acetyl-methionine,[11] and for *S*-methylglutathione[44]). For $S\therefore N^+$ radical cations the only values that we have concern deprotonated species identified by conductivity measurements. For instance at neutral pH in *S*-methylglutathione the peak at 390 nm was attributed to a S∴N radical[46] in which S is intramolecularly linked to N of the amine function. As for $S\therefore O^+$ radical cations, experimental data were obtained with various thioether systems (see references in ref 16). For instance, $S\therefore O^+$ radical cations absorb at 380−400 nm in 2-methylsulfanyl-benzoate,[47] at 410 nm in 3-methylsulfanyl-propionate[6], at 400 nm in (carboxyalkyl) thiopropionate,[10,48] and at 390 nm at low pH in *S*-methylglutathione. When looking globally at our results (Figure 3), one observes the absorption maxima of the $S\therefore O^+$ radical cations in both media (vacuum and water) and of some $S\therefore N^+$ in vacuum are in a large range of values, from 300 to 450 nm. Moreover most of the $S\therefore N^+$ compounds absorb at larger wavelengths, from 450 to 520 nm. The $S\therefore S^+$ radicals absorb even farther in the visible region. The experimentally observed large bands might hide several maxima corresponding to a population of radicals like those that we have identified.

Finally, the fate of these various radicals is not yet known. The only final compound that was isolated up to now in peptides is methionine sulfoxide. It is well-known that it can exist in two configurations "*R*" and "*S*" and that the configuration is important for the regeneration of methionine.[49] The mechanism involves an oxygen addition on the sulfur atoms. If the energy barrier between two enantiomers of the precursor radical cation would be high, one can make the hypothesis that the final stereoisomer would be determined by the geometry of the initial radical. As an example, GlyMetSN5pep2 and GlyMetSN5pep1 (the most stable conformations for Gly Met) would give rise both to the *S*-enantiomer. The formation of the 2c-3e bond would then be at the origin of the stereospecificity of the formation of methionine sulfoxide.

**Acknowledgment.** We thank IDRIS for computer time (project 040268-060268) and CCR (Université Paris VI, Paris, France). C.H.L. is indebted to the COST CM0603 action for fruitful discussions.

**Supporting Information Available:** Detailed definitions of the AIM and ELF topological signatures of the two-center three-electron bond. This information is available free of charge via the Internet at http://pubs.acs.org.

## References and Notes

(1) Vogt, W. *Free Radical Biol. Med.* **1995**, *18*, 93–105.
(2) Oiena, D. B.; Moskovitz, J. *Curr. Top. Dev. Biol.* **2007**, *80*, 93–133.
(3) Levine, R. L.; Berlett, B. S.; Moskovitz, J.; Mosoni, L.; Stadtman, E. R. *Mech. Ageing Dev.* **1999**, *107*, 323–332.
(4) Butterfield, A. D. *Chem. Res. Toxicol.* **1997**, *10*, 495.
(5) Dalle-Donne, I.; Rossi, R.; Giustarini, D.; Gagliano, N.; Di Simplicio, P.; Colombo, R.; Milzani, A. *Free Radical Biol. Med.* **2002**, *32*, 927–937.
(6) Clark, T. In *Sulfur-centered reactive intermediates in Chemistry and Biology.*; Chatgilialoglu, C., Asmus, D., Eds.; NATO-ASI Series, vol. 197; Plenum Press: New York, 1990; pp 13−18.
(7) Asmus, K. D. In *Radiation Chemistry, present status and future trends*; Jonah, C. D., Rao, M. B. S., Eds.; Elsevier Science: Amsterdam, The Netherlands, 2001; pp 341−393.
(8) Mieden, O. J.; Von Sonntag, C. *Z. Naturforsch.* **1989**, *44b*, 959–974. Schöneich, C.; Bobrowksi, K. *J. Am. Chem. Soc.* **1993**, *115*, 6538–6547.
(9) Holcman, J.; Bobrowski, K.; Schöneich, C.; Asmus, K. D. *Radiat. Phys. Chem.* **1991**, *37*, 473–478.
(10) Bobrowski, K.; Hug, G. L.; Marciniak, B.; Miller, B. L.; Schöneich, C. *J. Am. Chem. Soc.* **1997**, *119*, 8000–8011.
(11) Pogocki, D.; Schöneich, C. *J. Org. Chem.* **2002**, *67*, 1526–1535.
(12) Brunelle, P.; Rauk, A. *J. Phys. Chem. A* **2004**, *108*, 11032–11041.
(13) Brunelle, P.; Schöneich, C.; Rauk, A. *Can. J. Chem.* **2006**, *84*, 893–904.
(14) Pogocki, D.; Serdiuk, K.; Schöneich, C. *J. Phys. Chem. A* **2003**, *107*, 7032–7042.
(15) Hug, G. L.; Bobrowski, K.; Pogocki, D.; Hörner, G.; Marciniak, B. *ChemPhysChem* **2007**, *8*, 2202–2210.
(16) Glasss, R. S.; Hug, G. L.; Schoneich, C.; Wilson, G. S.; Kusnetsova, L.; Lee, T. M.; Ammam, M.; Lorance, E.; Nauser, T.; Nichol, G. S.; Yamamoto, T. *J. Am. Chem. Soc.* **2009**, *131*, 13791–13805.
(17) Aslangul, C.; Constanciel, R.; Daudel, R.; Kottis, P. , *Advances in Quantum Chemistry*; Lödwin, P.-O., Ed.; Academic Press: New York, 1972; Vol. 6, pp 93−141.

(18) Abraham, R.; Marsden, J. E. *Dynamics and the Geometry of Behavior*; Adison-Wesley: Reading, MA, 1992.

(19) Bader, R. F. W. *Atoms in Molecules: a Quantum Theory*; Oxford University Press: Oxford, U.K., 1990.

(20) Silvi, B.; Savin, A. *Nature* **1994**, *371*, 683.

(21) Haüssermann, U.; Wengert, S.; Nesper, R. *Angew. Chem., Int. Ed. Engl.* **1994**, *33*, 2073.

(22) Becke, A. D.; Edgecombe, K. E. *J. Chem. Phys.* **1990**, *92*, 5397.

(23) The ELF topological analysis provides a partition of the molecular space into basins of attractors (the local maxima of ELF) which are of two kinds: on the one hand the core basins noted C(X) which encompass the nuclei X with $Z > 2$, and on the other hand the valence basins V(X, Y, . . .) (Y = another atom) which fill the remaining space. The valence basins are characterized by their synaptic order, i.e., the number of core basins with which they share a common separatrix. Monosynaptic basins thus correspond to conventional lone pairs, disynaptic basins to two-center bonds, and polysynaptic basins to multicenter bonds.

(24) Lewis, G. N. *J. Am. Chem. Soc.* **1916**, *38*, 762.

(25) Lewis, G. N. *Valence and the Structure of Atoms and Molecules*; Dover: New York, 1966.

(26) Fourré, I.; Bergès, J.; Braïda, B.; Houée-Levin, C. *Chem. Phys. Lett.* **2008**, *467*, 164–169.

(27) Braïda, B.; Hiberty, P.; Savin, A. *J. Phys. Chem. A* **1998**, *102*, 7872.

(28) Drew, A.; Head-Gordon, M. *Chem. Rev.* **2005**, 4009.

(29) Frisch, M. J.; Trucks, G. W.; Schlegel, H. B.; Scuseria, G. E.; Robb, M. A.; Cheeseman, J. R.; Montgomery, J. A., Jr.; Vreven, T.; Kudin, K. N.; Burant, J. C.; Millam, J. M.; Iyengar, S. S.; Tomasi, J.; Barone, V.; Mennucci, B.; Cossi, M.; Scalmani, G.; Rega, N.; Petersson, G. A.; Nakatsuji, H.; Hada, M.; Ehara, M.; Toyota, K.; Fukuda, R.; Hasegawa, J.; Ishida, M.; Nakajima, T.; Honda, Y.; Kitao, O.; Nakai, H.; Klene, M.; Li, X.; Knox, J. E.; Hratchian, H. P.; Cross, J. B.; Bakken, V.; Adamo, C.; Jaramillo, J.; Gomperts, R.; Stratmann, R. E.; Yazyev, O.; Austin, A. J.; Cammi, R.; Pomelli, C.; Ochterski, J. W.; Ayala, P. Y.; Morokuma, K.; Voth, G. A.; Salvador, P.; Dannenberg, J. J.; Zakrzewski, V. G.; Dapprich, S.; Daniels, A. D.; Strain, M. C.; Farkas, O.; Malick, D. K.; Rabuck, A. D.; Raghavachari, K.; Foresman, J. B.; Ortiz, J. V.; Cui, Q.; Baboul, A. G.; Clifford, S.; Cioslowski, J.; Stefanov, B. B.; Liu, G.; Liashenko, A.; Piskorz, P.; Komaromi, I.; Martin, R. L.; Fox, D. J.; Keith, T.; Al-Laham, M. A.; Peng, C. Y.; Nanayakkara, A.; Challacombe, M.; Gill, P. M. W.; Johnson, B.; Chen, W.; Wong, M. W.; Gonzalez, C.; and Pople, J. A. *Gaussian 03, Revision C.02.*; Gaussian, Inc.: Wallingford, CT, 2004.

(30) Fourré, I.; Silvi, B. *Heteroat. Chem.* **2007**, *18*, 135.

(31) Silvi, B.; Fourré, I.; Alikhani, M. E. *Monatsh. Chem.* **2005**, *136*, 855.

(32) *The Quantum Theory of Atoms in Molecules: From Solid State to DNA and Drug Design*; Matta, S. C.; Boyd, R. J., Eds. Wiley-VCH: Weinheim 2007.

(33) Silvi, B.; Pilme, J.; Fuster, F.; Alikhani, M. E. In *Metal-Ligand Interactions: Molecular, Nano, Micro, and Macro-Systems in Complex Environments*; Russo, N., et al., Eds.; Kluwer Academic Publishers: Dordrecht, 2003; pp 241−284.

(34) Bergès, J.; Fuster, F.; Jacquot, J.-P.; Silvi, B.; Houée-Levin, C. *Nukleonika* **2000**, *45*, 23.

(35) Fourré, I.; Silvi, B.; Sevin, A.; Chevreau, H. *J. Phys. Chem. A* **2002**, *106*, 2561–2571.

(36) Fourré, I.; Bergès, J. *J. Phys. Chem. A* **2004**, *108*, 898–906.

(37) Llusar, R.; Beltrán, A.; Andrés, J.; Fuster, F.; Silvi, B. *J. Phys. Chem. A* **2001**, *105*, 9460–9466.

(38) Fradera, X.; Austen, M. A.; Bader, R. F. W. *J. Phys. Chem. A* **1999**, *103*, 304–314.

(39) Savin, A.; Silvi, B.; Colonna, F. *Can. J. Chem.* **1996**, *74*, 1088–1096.

(40) Fuster, F.; Silvi, B. *Theor. Chem. Acc.* **2000**, *104*, 13–21.

(41) Pauling, L. *J. Am. Chem. Soc.* **1931**, *53*, 3225.

(42) Bergès, J.; Varmenot, N.; Scemama, A.; Abedinzadeh, Z.; Bobrowski, K. *J. Phys. Chem. A.* **2007**, *112*, 7015.

(43) Bobrowski, K.; Hug, Gordon L.; Pogocki, D.; Marciniak, B.; Schöneich, C. *J. Phys. Chem. B* **2007**, *111*, 9608–9620.

(44) Varmenot, N.; Bergès, J.; Abedinzadeh, Z.; Scemama, A.; Strzelczak, G.; Bobrowski, K. *J. Phys. Chem. A* **2004**, *108*, 6331–6346.

(45) Bobrowski, K.; Hug, G. L.; Pogocki, D.; Marciniak, B.; Schöneich, C. *J. Am. Chem. Soc.* **2007**, *129*, 9236–9245.

(46) Schöneich, C.; Zhao, F.; Madden, K. P.; Bobrowski, K. *J. Am. Chem. Soc.* **1994**, *116*, 4641–4652.

(47) Chatgilialoglu, C.; Castelhano, A. L.; Griller, D. *J. Org. Chem.* **1985**, *50*, 2516.

(48) Bobrowski, K.; Pogocki, D.; Schöneich, C. *J. Phys. Chem. A* **1998**, *102*, 10512–10521.

(49) Hansel, A.; Heinemann, S. H.; Hoshi, T. *Biochim. Biophys. Acta* **2005**, *1703*, 239–247.

JP911983A